

Experimental superposition of time directions

Teodor Strömberg,^{1,*} Peter Schiansky,¹ Marco Túlio Quintino,^{2,3,4} Michael Antesberger,¹ Lee Rozema,² Iris Agresti,² Časlav Brukner,^{3,2} and Philip Walther^{2,†}

¹University of Vienna, Faculty of Physics & Vienna Doctoral School in Physics, Boltzmannngasse 5, A-1090 Vienna, Austria

²University of Vienna, Faculty of Physics & Research Network Quantum

Aspects of Space Time (TURIS), Boltzmannngasse 5, 1090 Vienna, Austria

³Institute for Quantum Optics and Quantum Information, Boltzmannngasse 3, 1090 Vienna, Austria

⁴Sorbonne Université, CNRS, LIP6, F-75005 Paris, France

In the macroscopic world, time is intrinsically asymmetric, flowing in a specific direction, from past to future. However, the same is not necessarily true for quantum systems, as some quantum processes produce valid quantum evolutions under time reversal. Supposing that such processes can be probed in both time directions, we can also consider quantum processes probed in a coherent superposition of forwards and backwards time directions. This yields a broader class of quantum processes than the ones considered so far in the literature, including those with indefinite causal order. In this work, we demonstrate for the first time an operation belonging to this new class: the quantum time flip. Using a photonic realisation of this operation, we apply it to a game formulated as a discrimination task between two sets of operators. This game not only serves as a witness of an indefinite time direction, but also allows for a computational advantage over strategies using a fixed time direction, and even those with an indefinite causal order.

INTRODUCTION

In recent years, the framework of quantum theory has been generalised to describe agents interacting through quantum processes with indefinite causal orders [1–3]. These processes have been realised experimentally using photonic platforms [4–8], thereby witnessing the implementation of causally non-separable series of events. Remarkably, these are not the most general processes allowed by quantum mechanics. Take, for example, the quantum SWITCH [2]: even though the causal order of the constituent events is indefinite, each operation is accessed only in a single time direction. By considering processes where the time direction of the underlying operations is indefinite, one can go beyond the framework of indefinite causality. Indeed, a quantum superposition of evolutions with opposite thermodynamic arrows of time was first proposed in [9]. By associating the “forwards” temporal direction with a positive change in the entropy generated in a thermodynamic process, and its “time-reversing” counterpart with a negative change, the corresponding superposition of processes exhibits a quantum-mechanically undefined thermodynamic arrow of time.

More generally, processes with an indefinite time direction can be studied by considering operations that exhibit a time symmetry; these operations admit a change of reference frame that yields a valid quantum evolution in which the time coordinate is inverted.

Unitary channels are an example of such operations, and in particular they admit the following time-reversal symmetries: for every evolution U , both the inverse $U \rightarrow U^\dagger$ and the transpose $U \rightarrow U^T$ are valid time-reversal operations.

Given quantum operations that can in principle be accessed in both time directions, we can consider coherent superpositions of transformations made in the forwards and backwards time-directions. This amounts to a new kind of process, which we will refer to as being *inseparable in the arrow of time*, an example of which - called the *quantum time flip* - was recently introduced in Ref. [10]. This process cannot be realised within the quantum circuit model. In this work we nevertheless present a photonic implementation of the quantum time flip by exploiting *device dependent symmetries* of our experimental apparatus. A quantum state undergoing a time evolution is encoded in the polarization degree of freedom of a single photon, while a control qubit determining the time direction is encoded in its path degree of freedom. We show that polarization operations with waveplates naturally implement different time directions for forwards and backwards propagation directions through the waveplates, given the correct Stokes-parameter convention. This results in a deterministic time-reversal, in contrast to more general approaches which may involve multiple uses of the input operation in combination with probabilistic or non-exact methods [11–20]. We can furthermore realise the quantum time flip deterministically by passing the photon through the waveplates in a superposition of the two propagation directions.

We certify the indefinite time direction by demon-

* Corresponding author: teodor.stroemberg@univie.ac.at

† Corresponding author: philip.walther@univie.ac.at

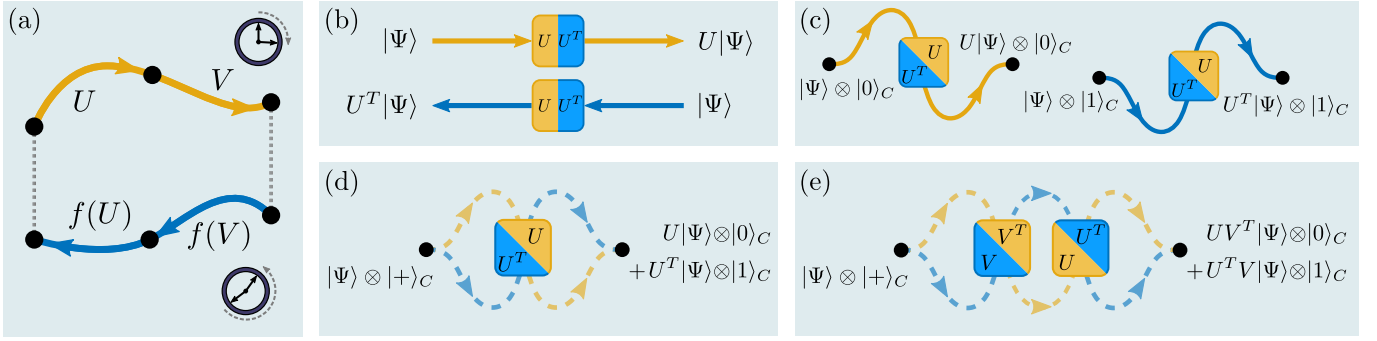


FIG. 1. **Time-reversal and the quantum time flip.** (a) The forwards (top) and backwards (bottom) directions of the same time-evolution are shown in yellow and blue, respectively. The backwards time-evolution is given by some function f of the forwards evolution, and decomposing the total time evolution into steps shows that f must be order reversing. The inverse and transpose are examples of such order reversing functions. (b) Quantum gates are often modelled as black boxes with an input and an output. In this work, we consider black boxes that can be accessed in two different directions, producing either the forwards or backwards time-evolution depending on which direction the box is accessed in. Here, the backwards time-evolution is taken to be the transpose. (c) A control degree of freedom can be introduced to control in which direction the black box is accessed. (d) By putting the control qubit in a coherent superposition of the two states in (c) the box is accessed in a superposition of both directions, and the input state is propagated in a superposition of time directions. This is a realisation of the quantum time flip. (e) The quantum time flip can be applied to more than a single gate. This figure illustrates a scenario where two gates are accessed in a superposition of orders, in which they always have the opposite time directions. As described in the main text, this use of two quantum time flips can yield a computational advantage.

strating an information-theoretic advantage of the quantum time flip in the context of a computational game. In this setting, the quantum time flip not only outperforms strategies that utilise operations with a fixed time direction, but even strategies that exploit operations with an indefinite causal order [4, 21].

QUANTUM CIRCUITS, UNITARY TRANSPOSITION, AND PROCESSES WITH INDEFINITE TIME DIRECTION

The standard quantum circuit formalism provides solid grounds for quantum computing and forms the basis for quantum complexity theory [22, 23]. However, it also imposes limitations on how we apply quantum theory. In a circuit, operations necessarily respect a definite causal order and the strict notion of input and output. The existence of time reversal processes such as unitary transposition is forbidden by the standard circuit formalism when given access to one [15, 16] or even two [10] uses of an unknown unitary. However, for practical and foundational reasons, researchers have been designing and pursuing non-exact and probabilistic schemes aimed towards this goal [11–19]. Remarkably, a very recent work shows that in the qubit case, when four uses of the input operation are available, there exists a quantum circuit to invert arbitrary unitary operations [20].

In quantum theory, reversible operations are de-

scribed by unitary operators. Processes which reverse a composition of such operations may be expressed by a function f satisfying:

$$f(UV) = f(V)f(U), \quad \forall U, V, \quad (1)$$

for all unitary operators U and V (see Fig. 1). Under natural assumptions, it can be proven that, up to a unitary transformation, there are only two time reversal functions f , unitary transposition $f(U) = U^T$ and unitary inversion $f(U) = U^{-1}$ [10]. For two-dimensional systems, unitary transposition and unitary inversion are unitarily equivalent via a Pauli σ_Y operation. This follows from the identity, $U^{-1} = \sigma_Y U^T \sigma_Y$ which holds for all operators $U \in SU(2)$. Hence, for qubits, universal unitary transposition is possible if and only if unitary inversion is possible. When focusing on a particular physical implementation, the general aspects of the standard quantum circuit formalism may limit our view and lead to an apparent mismatch between theory and practice. A known illustrative example is the universal coherent control of unitary operations, where an arbitrary unitary U is applied to the target system conditional on the state of a control qubit: $U \mapsto \mathbb{1} \otimes |0\rangle\langle 0|_C + U \otimes |1\rangle\langle 1|_C$. While it is not possible to design a quantum circuit to perform universal control, a simple Mach-Zehnder optical interferometer can be used for this task [24–26]. Indeed, experimental control of black box quantum gates has been demonstrated [27, 28]. Such experimental implementations exploit the knowledge of the position of the physical device per-

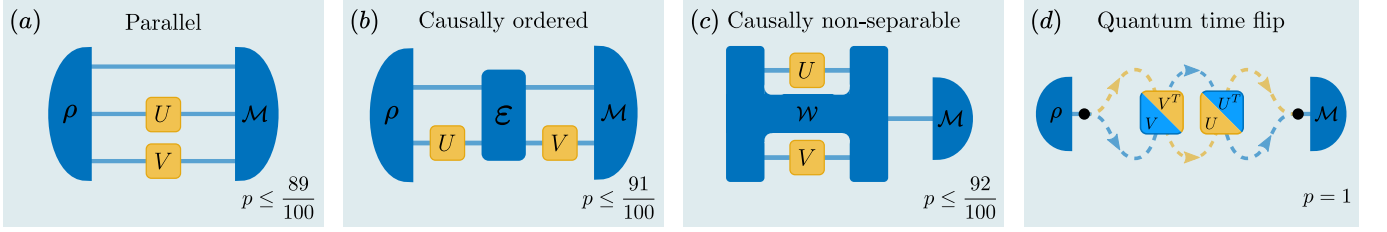


FIG. 2. **Classes of game strategies.** The figure depicts different strategies for the game described in the main text and their corresponding maximum winning probabilities p . These strategies differ in how they are able to access the gates picked by the referee. The strategies (a)-(c) are shown here in the forwards time direction, but are also valid in the backwards time direction in which both gates are transposed. Each subsequent strategy is strictly better than the previous one, and only players who have access to a quantum time flip process can win the game with unity probability. **(a)** Parallel gate order. **(b)** Causally ordered gate sequence. **(c)** Process without a definite causal order. **(d)** Quantum time flip.

forming the gate, circumventing this apparent limitation imposed by the quantum circuit formalism.

Although time reversal processes such as unitary transposition are not possible within the standard circuit formalism when given access to one [15, 16] or even two [10] uses of an unknown unitary, in this work we implement general qubit unitary transposition, as well as the quantum time flip process, using a particular optical construction. Similar to the case of universal coherent control, we make use of knowledge about our specific experimental apparatus and realise a gadget implementing an arbitrary unitary U which may be used in two different directions. In the ‘forwards’ direction, this gadget implements the standard U , while in the ‘backwards’ one it has the effect of the transposed operation U^T .

Moreover, in addition to “simply” reversing a quantum evolution, we also coherently superpose the forwards and backwards time evolutions, and in so doing perform an optical implementation of a process with an indefinite time direction [10], i.e. one which cannot be described as a convex mixture of processes where time flows forwards and processes where time flows backwards. The process that we implement optically is the quantum time flip for unitary transposition, a process which acts on unitary operations as:

$$U \mapsto U \otimes |0\rangle\langle 0|_C + U^T \otimes |1\rangle\langle 1|_C. \quad (2)$$

We then compose the time flip process of Eq. (2) with its flipped version, $V \mapsto V^T \otimes |0\rangle\langle 0|_C + V \otimes |1\rangle\langle 1|_C$, to obtain a process which acts on a pair of unitary operators as:

$$(U, V) \mapsto UV^T \otimes |0\rangle\langle 0|_C + U^T V \otimes |1\rangle\langle 1|_C. \quad (3)$$

In addition to having an indefinite time direction, the process described in Eq. (3) cannot be described by general process matrices with indefinite causality such as the quantum switch [2] or the Oreshkov-Costa-Brukner

(OCB) process [3]. In the next section, we will explain how to witness this property.

GAME DESCRIPTION

We now describe a discrimination task, first introduced in Ref. [10], where the quantum time flip process will be used as a resource to increase our performance. In this game, a referee provides the player with two black box unitaries, U and V , belonging to either the set \mathcal{M}_+ or \mathcal{M}_- , which are known to respect the property:

$$\mathcal{M}_+ := \{(U, V) : UV^T = +U^T V\} \quad (4)$$

$$\mathcal{M}_- := \{(U, V) : UV^T = -U^T V\}. \quad (5)$$

The player is then challenged to determine which of the two sets the gates were picked from, while only being allowed to access each of the black boxes once.

As discussed in the previous section, a player able to perform the quantum time flip may implement the process:

$$(U, V) \mapsto UV^T \otimes |0\rangle\langle 0|_C + U^T V \otimes |1\rangle\langle 1|_C. \quad (6)$$

Consider as a strategy an initial state of the form $|\psi\rangle_T \otimes |+\rangle_C$, where $|\pm\rangle_C = \frac{|0\rangle_C \pm |1\rangle_C}{\sqrt{2}}$, $|\psi\rangle$ is an arbitrary state, and the subscripts C and T refer to the control and target qubits. Sending this state through the gate in Eq. (6) gives the state:

$$\left[\frac{UV^T + U^T V}{2} \right] |\psi\rangle_T |+\rangle_C + \left[\frac{UV^T - U^T V}{2} \right] |\psi\rangle_T |-\rangle_C. \quad (7)$$

Since the states $|\pm\rangle$ are orthogonal, a player using this strategy can always correctly determine which set was chosen by the referee. In contrast, players who do not have access to indefinite time strategies may not be able

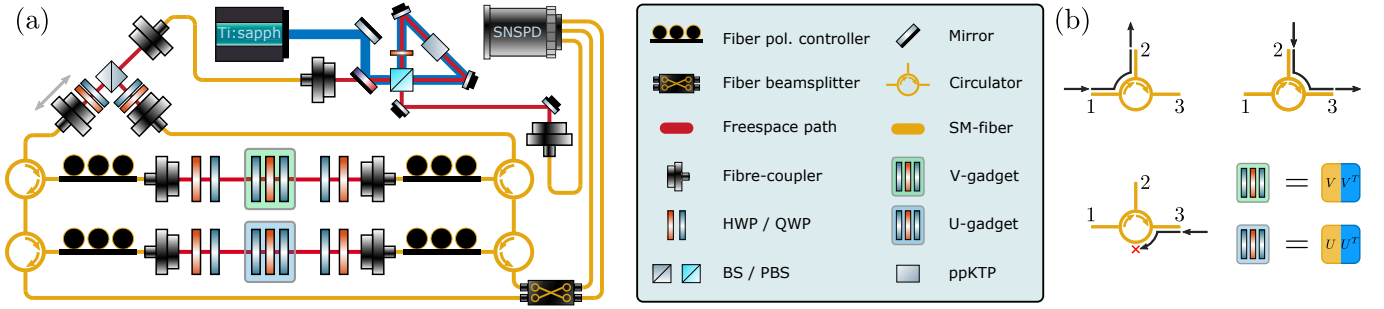


FIG. 3. **Experimental apparatus.** (a) A type-II spontaneous parametric down-conversion source generates frequency degenerate single-photon pairs at 1546 nm in a ppKTP crystal (top). The signal photon is sent to a heralding detector, while the idler photon is routed to a balanced bulk beam-splitter and coupled into single-mode fiber. A piezo-electric actuator attached to one of the fiber couplers allows for control over the interferometric phase, and pairs of HWPs / QWPs are used for polarization compensation through the fibers. After the initial beam-splitter two fiber circulators guide the photon through the V-gadget. Propagating through the gadget in the ‘forwards’ direction implements the unitary V , while propagating ‘backwards’ has the effect of applying the transposed operation relative to the ‘forward’ direction. One of the two paths through first the gadget therefore results in the V^T being applied instead of V . Two additional circulators then route the photon through a gadget implementing U (U^T) in ‘forwards’ (‘backwards’) direction. Finally, the signal photon is sent to a fiber beam-splitter, which applies a Hadamard gate on the path degree of freedom, and correlates the two spatial output modes with the sets \mathcal{M}_+ , \mathcal{M}_- . Detection is performed by superconducting nanowire single-photon detectors (SNSPDs) housed in a 1 K cryostat. Additional QWP/HWP pairs are used to compensate fiber-induced polarization rotations. (b) The fiber circulators route the light from port 1 \rightarrow 2, from 2 \rightarrow 3 and block light entering in port 3. The bidirectional boxes in Fig. 1 are realised using sets of three waveplates. Depending on the propagation direction, they implement either the unitary operation U/V or U^T/V^T .

to ascertain with certainty to which set a given pair of unitaries (U, V) belongs. In order to make this claim concrete, Ref. [10] considers a particular game where the set \mathcal{M}_+ has 13 pairs of unitary operators respecting $UV^T = +U^TV$, and \mathcal{M}_- has 8 pairs of unitary operators respecting $UV^T = -U^TV$; these two sets of unitary operators are presented in the Methods. Here, we consider an average case variation of the aforementioned game, which goes as follows: with uniform probability $p = \frac{1}{13+8}$, the referee picks a pair of unitary operators (U, V) from \mathcal{M}_+ or \mathcal{M}_- and lets the player make a single use of each. We then consider the optimal success probability of players who have access to different kinds of resources. As indicated by Eq. (7), players who have access to the quantum time flip can always win with unity probability. The three other classes of strategies, shown in Fig. 2, only have access to a single time direction, forwards or backwards, and convex combinations of these strategies will be called separable in the arrow of time; a detailed mathematical characterisation of these strategies is presented in the methods. Employing the computer-assisted proof methods of Ref. [29] we obtain upper bounds on the maximal success probabilities for players restricted to particular classes of strategies. The code for this is openly available in our online repository, see Methods for details.

The first alternative strategy we consider is one in which the player is restricted to using U and V in parallel, and this results in a maximal success probability

that is bounded by $\frac{88}{100} \leq p_{\text{par}} \leq \frac{89}{100}$. Next, we consider players restricted to causally ordered strategies, whose maximal success probability is found to be bounded by $\frac{90}{100} \leq p_{\text{causal}} \leq \frac{91}{100}$. Finally, players given access to process matrices with indefinite causality (also called indefinite testers [30]), but with definite time direction, have their maximal success probability bounded by $\frac{91}{100} < p_{\text{i.c.}} \leq \frac{92}{100}$. This game is hence an example of a channel discrimination task with strict hierarchy between four different classes of strategies. Additionally, while the operations selected by the referee are treated as being fully characterised in the above analysis, there are no assumptions made about the measurements performed by the player, and these can be chosen freely. This is therefore an example of a semi-device-independent certification of an indefinite causal order [31, 32] and indefinite time direction.

EXPERIMENT

Our photonic implementation of the game described in the previous section makes use of the quantum time-flip strategy from Eq. (7) to achieve a success probability exceeding that of any strategy only using the gates in one time direction. To coherently apply the quantum time flip, we employ polarization optics in a partially common-path interferometer, depicted in Fig. 3, with the control and target qubits being encoded in the path

and polarization degrees of freedom of a single-photon, respectively. Our experiment makes use of two quantum time flips, sequentially applied to the two unitaries V and U . The resulting controlled channel is the one of Eq. (7) where the gates UV^T and U^TV act on the target (polarization) qubit and are implemented using two Simon-Mukunda polarization gadgets consisting of three waveplates each [33], for which the transpose operation is obtained by reversing the propagation direction.

Such polarization gadgets generally do not realise the transpose operation in the backwards propagation direction, but rather a related operation:

$$U_{\text{fw}} \rightarrow U_{\text{bw}} = PU_{\text{fw}}^T P^\dagger, \quad (8)$$

where P is a matrix describing the change of reference frame to the backwards direction, and the subscripts indicate the propagation direction. While it is possible to construct a gadget that implements the transpose by introducing time-reversal symmetry breaking elements (T. Strömberg, R. Peterson, and P. Walther, SU(2) gadgets for counterpropagating polarization optics, Manuscript under preparation), here we instead exploit the fact that the transpose is a basis-dependent operation. More concretely, by adopting the convention $(S_1, S_2, S_3) \leftrightarrow (-Z, -Y, -X)$ for our Stokes parameters [34] we find that $P = \mathbb{1}$, and the polarization gadgets transform as the transpose under counterpropagation (see Methods). Superimposing two propagation directions through a gadget therefore allows us to implement the quantum time flip, with the photon path acting as a control degree of freedom. The specific coherent superposition of time flips in Eq. (3) is achieved through the use of fiber optic circulators.

The optical circuit in Fig. 3 begins with a bulk beam-splitter that initializes the control qubit into the state $|+\rangle_C = \frac{1}{\sqrt{2}}(|0\rangle_C + |1\rangle_C)$, after which two fiber circulators guide the photons through the V gadget in two different directions, giving the joint control-target state:

$$\frac{1}{\sqrt{2}}(V|\psi\rangle_T \otimes |0\rangle_C + V^T|\psi\rangle_T \otimes |1\rangle_C). \quad (9)$$

Entering the circulators from a different port, the photons are then directed to the U gadget, which they once again propagate through in opposite directions, transforming the joint state to:

$$\frac{1}{\sqrt{2}}(U^TV|\psi\rangle_T \otimes |0\rangle_C + UV^T|\psi\rangle_T \otimes |1\rangle_C). \quad (10)$$

At the end of the optical circuit, a fiber beam-splitter applies a Hadamard gate on the control qubit, giving the state:

$$\left[\frac{UV^T + U^TV}{2}\right]|\psi\rangle_T |+\rangle_C + \left[\frac{UV^T - U^TV}{2}\right]|\psi\rangle_T |-\rangle_C. \quad (11)$$

A projective measurement on the control (path) qubit in the computational basis then reveals whether (U, V) belong to \mathcal{M}_+ or \mathcal{M}_- .

The partially common-path structure of the interferometer has two distinct advantages: (1) photons in the two different propagation directions of the interferometer hit exactly the same spots on the waveplates and the physical symmetries of the gadget therefore ensures the faithful implementation of the time flip independently of any imperfections in the waveplates, (2) the paths traversed in both directions do not contribute any phase noise to the interferometer, thereby simplifying the phase stabilization. More specifically, only the paths connecting the two beam-splitters with the fiber circulators, as well as the fibers directly between the circulators, add phase noise to the interferometer. These fiber components, as well as the bulk beam-splitter at the interferometer input, are housed in a thermally and acoustically insulated box. The passive stabilization of these elements is sufficient to bring the phase drift down to a value of approximately 10 mrad min^{-1} . The use of a bulk-beamsplitter at the input was chosen in order to balance the losses induced by the fiber circulators through the free-space to fiber coupling, and to give control over the interferometer phase through a piezo-electric actuator, while the fiber beam-splitter at the output ensures perfect spatial mode overlap for high interferometric visibility.

RESULTS

Before demonstrating the quantum time flip in the context of the game, we first verified the ability of a polarization gadget to implement both a unitary and its transpose simultaneously, in the two different propagation directions of the light. To this end, we performed quantum process tomography on the implemented unitaries from the sets \mathcal{M}_+ and \mathcal{M}_- , in both propagation directions. We then compared the fidelity $\mathcal{F} = \langle (U_{\text{fw}}|\Psi\rangle)^\dagger U_{\text{bw}}^T |\Psi\rangle \rangle_{|\Psi\rangle}$ between the reconstructed unitaries in the forward direction, U_{fw} and V_{fw} , with the transposed reconstructed unitaries in the backwards direction, U_{bw}^T and V_{bw}^T (see Methods). The results of this are shown in Fig. 4, where the infidelity, defined as $1 - \mathcal{F}$, is plotted. The average infidelity is less than 10^{-3} , indicating that the gadgets correctly implement the unitaries and their transpose. Note that the fidelity of the transpose is independent of any errors in the retardance of the waveplates in the gadget itself. Such imperfections would cause the fidelity in the implementation of a desired unitary to drop, but would affect the forward and backward directions symmetrically. The

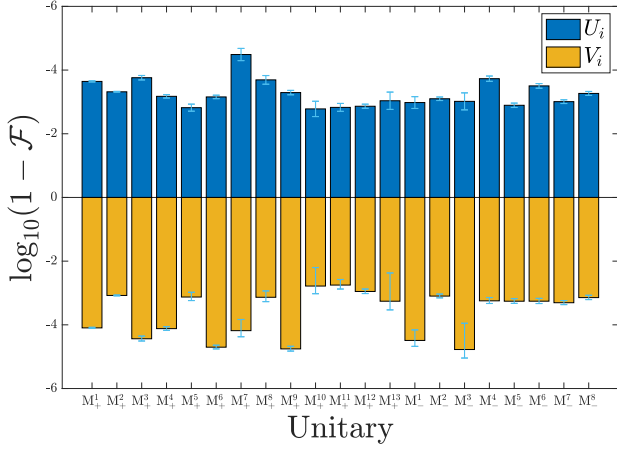


FIG. 4. **Unitary transposition infidelity.** The yellow and blue bars indicate the infidelity, $1 - \mathcal{F}$, of the unitaries U and V from the sets \mathcal{M}_+ and \mathcal{M}_- , measured in the forward propagation direction, with respect to the transpose of the reconstructed unitary measured in the backwards propagation direction. The standard deviation of the infidelities is shown in light blue. Higher bars indicate a lower infidelity, and therefore higher fidelity between the unitaries in the two propagation directions. The average infidelity is $7.9 \times 10^{-4} \pm 1.8 \times 10^{-5}$ indicating that the gadgets faithfully implement the transpose and the base unitary. The uncertainties were estimated using a Monte-Carlo simulation of the tomography accounting for errors in the waveplate angles. We attribute the residual errors to imperfect waveplate retardance in the tomography, and angle differences between the setting of the forwards and backwards unitaries, since in principle the gadgets perfectly implement the transpose of the unitary in the forward direction.

same is true for undesired offsets in the waveplate angles, however in the measurements shown in Fig. 4 the unitaries in the two directions were measured in separate runs, causing them to indeed be sensitive to waveplate angle errors, in addition to errors in the tomography itself.

Having verified the ability to implement a given unitary and its transpose with a single black box simultaneously, we then realised the game discussed in the previous sections. Using a single photon for every round of the game, a total of one million rounds were played. The data for the different elements of \mathcal{M}_+ and \mathcal{M}_- was collected sequentially to reduce the time spent rotating the waveplates. The game itself was played using the collected data by uniformly sampling from the two sets of unitaries (see Methods). The relative winning probabilities for each setting are shown in Fig. 5, where it can be seen that our implementation exceeds the indefinite tester bound of 0.92 for every setting, and by extension any strategy that is separable in the arrow of time. More specifically, the average winning probab-

ity is found to be 0.9945, with the best and worst case probabilities being 0.9993 and, 0.9860 respectively.

The formulation of the indefinite-time-direction witness as a game with only two outcomes, win or lose, allows for a straightforward statistical interpretation of the results. Since we have an upper bound on the probability of success for an indefinite tester, we can calculate the probability P of such a player having obtained v or more victories in N rounds:

$$P = \sum_{k=v}^N \binom{N}{k} p_{\text{i.c.}}^k (1 - p_{\text{i.c.}})^{N-k}. \quad (12)$$

This probability is exactly the P -value for the experimentally implemented process not being indefinite in its time direction. Out of the $N = 10^6$ rounds played in the experiment, $v = 994,512$ were won by successfully identifying the correct set, while 5,488 rounds were lost. Using a Chernoff bound tailored for the binomial distribution, we can provide an upper bound on the P -value, given by:

$$\sum_{k=v}^N \binom{N}{k} p_{\text{i.c.}}^k (1 - p_{\text{i.c.}})^{N-k} \leq \exp \left(-N D \left(\frac{v}{N} \parallel p_{\text{i.c.}} \right) \right), \quad (13)$$

where \exp is the exponential function and:

$$D \left(\frac{v}{N} \parallel p \right) := \frac{v}{N} \ln \left(\frac{v}{Np} \right) + \left(1 - \frac{v}{N} \right) \ln \left(\frac{1 - v/N}{1 - p} \right) \quad (14)$$

is the relative entropy. Direct calculation shows that $D \left(\frac{v}{N} \parallel p_{\text{i.c.}} \right) \approx 0.0627$, hence the P -value is upper bounded by $P \leq e^{-10^4}$, which is an extremely small number. We therefore conclude that a strategy with a definite time direction could not have produced as many wins as were observed, and the implemented process was inseparable in its arrow of time.

DISCUSSION

In this work we have demonstrated, for the first time, a process that is inseparable in the arrow of time. Using an optical interferometer, we implemented a coherent superposition of arbitrary unitary transformations and their time-reversal. Such a process can only be probabilistically simulated by a quantum circuit with a definite time direction. Even agents equipped with two copies of the gates and able to combine them in an indefinite order cannot realise the process deterministically, unless they are given the ability of pre- and post-selecting quantum systems [2, 35–40]. It is worth noting that our implementation of controlled unitary transposition is not in contradiction with the no-go theorem,

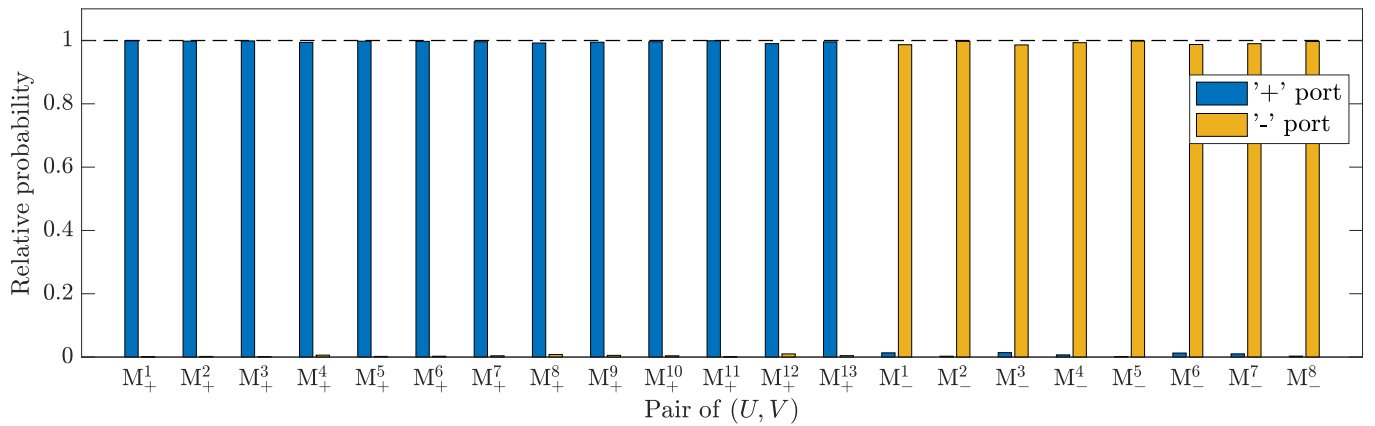


FIG. 5. **Experimental winning probabilities of the quantum flip game.** The figure shows the relative probability for a photon to exit in a given port of the interferometer for all the pairs of unitaries in the sets \mathcal{M}_+ and \mathcal{M}_- . For the gates in the set \mathcal{M}_+ the game is won when the photon exits in the '+' port (blue), whereas for the ones in the set \mathcal{M}_- the correct outcome is the '-' port. The observed average winning probability is 0.9945. Since the histogram corresponds to the actual number of times the different outcomes were recorded there is no associated uncertainty.

stating that there is no quantum circuit that can transform an unknown quantum unitary gate to its transpose [10, 15, 41]. Analogously to the impossibility of perfect unitary coherent control [10, 25, 28, 42], our implementation adopts a device that implements an arbitrary gate U , and while this gate can remain unknown, the physical device itself is neither arbitrary nor unknown. Indeed, it is the particular symmetries of the physical device that necessarily and deterministically generate the transposed gate U^T . Hence, in this context, our demonstration highlights the limitations of the quantum circuit model for describing the full range of quantum information processing protocols. Through a channel discrimination game, in which we outperform any strategy with a definite time direction, we furthermore certify that the coherent superposition of time-directions yields a process that is inseparable in its arrow of time.

Just as the study of indefinite causality led to the discovery and realisation of quantum information protocols with practical advantages [43, 44], we envision that future studies of processes with an indefinite time order will expand both the theoretical and experimental toolkit, and open up new avenues for quantum information processing. The experimental methods in this work could, for instance, be used to implement transposed circuits of higher dimension through the Reck scheme [45]. Finally, the investigation of time reversed quantum processes also holds applications in quantum thermodynamics. Indeed, in [10], it was shown that the processes for which the quantum time flip produces another valid process are exactly those which do not increase the entropy in either time direction, and the ap-

plication of superpositions of two time directions in the context of thermodynamic work was recently studied in [9, 46].

ACKNOWLEDGEMENTS

We thank Robert Peterson for fruitful discussions. This research was funded in whole, or in part, by the Austrian Science Fund (FWF) through [F7113] (BeyondC), [FG5] (Research Group 5) and [TAI 483]. For the purpose of open access, the author has applied a CC BY public copyright licence to any Author Accepted Manuscript version arising from this submission. M.T.Q. and C.B. acknowledge the Austrian Science Fund (FWF) through the SFB project BeyondC (sub-project F7103), a grant from the Foundational Questions Institute (FQXi) as part of the Quantum Information Structure of Spacetime (QISS) Project (qiss.fr). The opinions expressed in this publication are those of the authors and do not necessarily reflect the views of the John Templeton Foundation. This project has received funding from the European Union's Horizon 2020 research and innovation programme under the Marie Skłodowska-Curie grant agreement No 801110. It reflects only the authors' view, the EU Agency is not responsible for any use that may be made of the information it contains. ESQ has received funding from the Austrian Federal Ministry of Education, Science and Research (BMBWF).

AUTHOR CONTRIBUTIONS

T.S. and P.S. carried out the experiment and collected the data. T.S. and I.A. build the experimental setup. T.S., P.S. and M.T.Q. analysed the data. T.S. and P.S. designed the experiment. M.T.Q. carried out the computer assisted proofs. M.A. and L.R. conceived the experiment. P.W., C.B. and I.A. supervised the project. All authors contributed to writing the manuscript.

DATA AVAILABILITY

All data used in this work is openly available in Zenodo under: [10.5281/zenodo.7352614](https://zenodo.org/record/7352614)

CODE AVAILABILITY

The code used to perform the computer assisted proofs is openly available at the following online repository: <https://github.com/mtcq/UnitaryTransposition>

-
- [1] L. Hardy, Probability Theories with Dynamic Causal Structure: A New Framework for Quantum Gravity, arXiv e-prints , gr-qc/0509120 (2005), [arXiv:gr-qc/0509120](https://arxiv.org/abs/gr-qc/0509120) [gr-qc].
 - [2] G. Chiribella, G. M. D'Ariano, P. Perinotti, and B. Valiron, Quantum computations without definite causal structure, *Phys. Rev. A* **88**, 022318 (2013), [arXiv:0912.0195](https://arxiv.org/abs/0912.0195) [quant-ph].
 - [3] O. Oreshkov, F. Costa, and Č. Brukner, Quantum correlations with no causal order, *Nature Communications* **3**, 1092 (2012), [arXiv:1105.4464](https://arxiv.org/abs/1105.4464) [quant-ph].
 - [4] L. M. Procopio, A. Moqanaki, M. Araújo, F. Costa, I. Alonso Calafell, E. G. Dowd, D. R. Hamel, L. A. Rozema, Č. Brukner, and P. Walther, Experimental superposition of orders of quantum gates, *Nature Communications* **6**, 7913 (2015), [arXiv:1412.4006](https://arxiv.org/abs/1412.4006) [quant-ph].
 - [5] G. Rubino, L. A. Rozema, A. Feix, M. Araújo, J. M. Zeuner, L. M. Procopio, Č. Brukner, and P. Walther, Experimental verification of an indefinite causal order, *Science Advances* **3**, e1602589 (2017), [arXiv:1608.01683](https://arxiv.org/abs/1608.01683) [quant-ph].
 - [6] G. Rubino, L. A. Rozema, F. Massa, M. Araújo, M. Zych, Č. Brukner, and P. Walther, Experimental entanglement of temporal order, *Quantum* **6**, 621 (2022), [arXiv:1712.06884](https://arxiv.org/abs/1712.06884) [quant-ph].
 - [7] K. Goswami, C. Giarmatzi, M. Kewming, F. Costa, C. Branciard, J. Romero, and A. G. White, Indefinite Causal Order in a Quantum Switch, *Phys. Rev. Lett.* **121**, 090503 (2018), [arXiv:1803.04302](https://arxiv.org/abs/1803.04302) [quant-ph].
 - [8] G. Rubino, L. A. Rozema, D. Ebler, H. Kristjánsson, S. Salek, P. Allard Guérin, A. A. Abbott, C. Branciard, Č. Brukner, G. Chiribella, and P. Walther, Experimental quantum communication enhancement by superposing trajectories, *Physical Review Research* **3**, 013093 (2021), [arXiv:2007.05005](https://arxiv.org/abs/2007.05005) [quant-ph].
 - [9] G. Rubino, G. Manzano, and Č. Brukner, Quantum superposition of thermodynamic evolutions with opposing time's arrows, *Communications Physics* **4**, 1–10 (2021), [arXiv:2008.02818](https://arxiv.org/abs/2008.02818) [quant-ph].
 - [10] G. Chiribella and Z. Liu, Quantum operations with indefinite time direction, *Communications Physics* **5**, 190 (2022), [arXiv:2012.03859](https://arxiv.org/abs/2012.03859) [quant-ph].
 - [11] G. Chiribella and D. Ebler, Optimal quantum networks and one-shot entropies, *New Journal of Physics* **18**, 093053 (2016), [arXiv:1606.02394](https://arxiv.org/abs/1606.02394) [quant-ph].
 - [12] I. S. B. Sardharwalla, T. S. Cubitt, A. W. Harrow, and N. Linden, Universal Refocusing of Systematic Quantum Noise, ArXiv e-prints (2016), [arXiv:1602.07963](https://arxiv.org/abs/1602.07963) [quant-ph].
 - [13] M. Navascués, Resetting Uncontrolled Quantum Systems, *Phys. Rev. X* **8**, 031008 (2018), [arXiv:1710.02470](https://arxiv.org/abs/1710.02470) [quant-ph].
 - [14] M. T. Quintino, Q. Dong, A. Shimbo, A. Soeda, and M. Murao, Reversing Unknown Quantum Transformations: Universal Quantum Circuit for Inverting General Unitary Operations, *Phys. Rev. Lett.*, **123**, 210502 (2019), [arXiv:1810.06944](https://arxiv.org/abs/1810.06944) [quant-ph].
 - [15] M. T. Quintino, Q. Dong, A. Shimbo, A. Soeda, and M. Murao, Probabilistic exact universal quantum circuits for transforming unitary operations, *Phys. Rev. A* **100**, 062339 (2019), [arXiv:1909.01366](https://arxiv.org/abs/1909.01366) [quant-ph].
 - [16] M. T. Quintino and D. Ebler, Deterministic transformations between unitary operations: Exponential advantage with adaptive quantum circuits and the power of indefinite causality, *Quantum* **6**, 679 (2022), [arXiv:2109.08202](https://arxiv.org/abs/2109.08202) [quant-ph].
 - [17] D. Trillo, B. Dive, and M. Navascués, Translating Uncontrolled Systems in Time, *Quantum* **4**, 374 (2020), [arXiv:1903.10568](https://arxiv.org/abs/1903.10568) [quant-ph].
 - [18] D. Trillo, B. Dive, and M. Navascués, A universal quantum rewinding protocol with an arbitrarily high probability of success, arXiv e-prints (2022), [arXiv:2205.01131](https://arxiv.org/abs/2205.01131) [quant-ph].
 - [19] P. Schiavsky, T. Strömberg, D. Trillo, V. Saggio, B. Dive, M. Navascués, and P. Walther, Demonstration of universal time-reversal for quantum processes, arXiv e-prints (2022), [arXiv:2205.01122](https://arxiv.org/abs/2205.01122) [quant-ph].
 - [20] S. Yoshida, A. Soeda, and M. Murao, Reversing unknown qubit-unitary operation, deterministically and exactly, arXiv e-prints (2022), [arXiv:2209.02907](https://arxiv.org/abs/2209.02907) [quant-ph].
 - [21] M. M. Taddei, J. Cariñe, D. Martínez, T. García, N. Guerrero, A. A. Abbott, M. Araújo, C. Branciard, E. S. Gómez, S. P. Walborn, L. Aolita, and G. Lima, Computational advantage from the quantum superposition of multiple temporal orders of photonic gates, *PRX Quantum* **2**, 010320 (2021), [arXiv:2002.07817](https://arxiv.org/abs/2002.07817) [quant-ph].
 - [22] M. Nielsen and I. Chuang, *Quantum Computation and Quantum Information*, Cambridge Series on Information and the Natural Sciences (Cambridge University Press, 2000).
 - [23] J. Watrous, Quantum Computational Complexity, arXiv e-prints (2008), [arXiv:0804.3401](https://arxiv.org/abs/0804.3401) [quant-ph].

- [24] A. Soeda, Limitations on quantum subroutine designing due to the linear structure of quantum operators (2013).
- [25] M. Araújo, A. Feix, F. Costa, and Č. Brukner, Quantum circuits cannot control unknown operations, *New Journal of Physics* **16**, 093026 (2014), [arXiv:1309.7976 \[quant-ph\]](#).
- [26] A. Bisio, M. Dall’Arno, and P. Perinotti, Quantum conditional operations, *Phys. Rev. X* **94**, 022340 (2016), [arXiv:1509.01062 \[quant-ph\]](#).
- [27] X.-Q. Zhou, T. C. Ralph, P. Kalasuwan, M. Zhang, A. Peruzzo, B. P. Lanyon, and J. L. O’Brien, Adding control to arbitrary unknown quantum operations, *Nature Communications* **2**, 413 (2011), [arXiv:1006.2670 \[quant-ph\]](#).
- [28] J. Thompson, K. Modi, V. Vedral, and M. Gu, Quantum plug n’ play: modular computation in the quantum regime, *New Journal of Physics* **20**, 013004 (2018).
- [29] J. Bavaresco, M. Murao, and M. T. Quintino, Strict hierarchy between parallel, sequential, and indefinite-causal-order strategies for channel discrimination, *Phys. Rev. Lett.* **127**, 200504 (2021), [2011.08300 \[quant-ph\]](#).
- [30] G. Chiribella and D. Ebler, Quantum speedup in the identification of cause-effect relations, *Nature Communications* **10**, 1472 (2019), [arXiv:1806.06459 \[quant-ph\]](#).
- [31] J. Bavaresco, M. Araújo, Č. Brukner, and M. T. Quintino, Semi-device-independent certification of indefinite causal order, *Quantum* **3**, 176 (2019), [arXiv:1903.10526 \[quant-ph\]](#).
- [32] H. Cao, J. Bavaresco, N.-N. Wang, L. A. Rozema, C. Zhang, Y.-F. Huang, B.-H. Liu, C.-F. Li, G.-C. Guo, and P. Walther, Experimental semi-device-independent certification of indefinite causal order, *arXiv e-prints* (2022), [arXiv:2202.05346 \[quant-ph\]](#).
- [33] R. Simon and N. Mukunda, Minimal three-component $su(2)$ gadget for polarization optics, *Physics Letters A* **143**, 165–169 (1990).
- [34] N. J. Frigo, F. Bucholtz, G. A. Cranch, and J. M. Singley, On the choice of conventions in polarization evolution calculations and representations, *J. Lightwave Technol.* **40**, 179–190 (2022).
- [35] R. Oeckl, General boundary quantum field theory: Foundations and probability interpretation, *arXiv e-prints*, [hep-th/0509122](#) (2005), [arXiv:hep-th/0509122 \[hep-th\]](#).
- [36] O. Oreshkov and N. J. Cerf, Operational quantum theory without predefined time, *New Journal of Physics* **18**, 073037 (2016), [arXiv:1406.3829 \[quant-ph\]](#).
- [37] G. Chiribella, G. M. D’Ariano, P. Perinotti, and B. Valiron, Quantum computations without definite causal structure, *Phys. Rev. A* **88**, 022318 (2013), [arXiv:0912.0195 \[quant-ph\]](#).
- [38] R. Silva, Y. Guryanova, A. J. Short, P. Skrzypczyk, N. Brunner, and S. Popescu, Connecting processes with indefinite causal order and multi-time quantum states, *New Journal of Physics* **19**, 103022 (2017), [arXiv:1701.08638 \[quant-ph\]](#).
- [39] G. Svetlichny, Time Travel: Deutsch vs. Teleportation, *International Journal of Theoretical Physics* **50**, 3903–3914 (2011), [arXiv:0902.4898 \[quant-ph\]](#).
- [40] S. Lloyd, L. Maccone, R. Garcia-Patron, V. Giovannetti, Y. Shikano, S. Pirandola, L. A. Rozema, A. Darabi, Y. Soudagar, L. K. Shalm, and A. M. Steinberg, Closed Timelike Curves via Postselection: Theory and Experimental Test of Consistency, *Phys. Rev. Lett.* **106**, 040403 (2011), [arXiv:1005.2219 \[quant-ph\]](#).
- [41] G. Chiribella, E. Aurell, and K. Życzkowski, Symmetries of quantum evolutions, *Physical Review Research* **3**, 033028 (2021), [arXiv:2101.04962 \[quant-ph\]](#).
- [42] S. Nakayama, A. Soeda, and M. Murao, Universal construction of controlled-unitary gates using dynamical decoupling and the quantum zeno effect, *AIP Conference Proceedings* **1633**, 183–185 (2014), [https://aip.scitation.org/doi/pdf/10.1063/1.4903131](#).
- [43] P. Allard Guérin, A. Feix, M. Araújo, and Č. Brukner, Exponential Communication Complexity Advantage from Quantum Superposition of the Direction of Communication, *Physical review letters* **117**, 100502 (2016), [arXiv:1605.07372 \[quant-ph\]](#).
- [44] K. Wei, N. Tischler, S.-R. Zhao, Y.-H. Li, J. M. Arrazola, Y. Liu, W. Zhang, H. Li, L. You, Z. Wang, Y.-A. Chen, B. C. Sanders, Q. Zhang, G. J. Pryde, F. Xu, and J.-W. Pan, Experimental Quantum Switching for Exponentially Superior Quantum Communication Complexity, *Phys. Rev. Lett.* **122**, 120504 (2019), [arXiv:1810.10238 \[quant-ph\]](#).
- [45] M. Reck, A. Zeilinger, H. J. Bernstein, and P. Bertani, Experimental realization of any discrete unitary operator, *Physical review letters* **73**, 58 (1994).
- [46] G. Rubino, G. Manzano, L. A. Rozema, P. Walther, J. M. R. Parrondo, and Č. Brukner, Inferring work by quantum superposing forward and time-reversal evolutions, *Physical Review Research* **4**, 013208 (2022), [arXiv:2107.02201 \[quant-ph\]](#).
- [47] G. Chiribella, G. M. D’Ariano, and P. Perinotti, Theoretical framework for quantum networks, *Phys. Rev. A* **80**, 022339 (2009), [arXiv:0904.4483 \[quant-ph\]](#).
- [48] M. Ziman, Process positive-operator-valued measure: A mathematical framework for the description of process tomography experiments, *Phys. Rev. A* **77**, 062112 (2008), [arXiv:0802.3862 \[quant-ph\]](#).

METHODS

Arbitrary unitary transposition

The description of linear retarders depends on the convention used for the polarization states, i.e. which Pauli matrices are associated with which Stokes parameters. The most commonly used convention in quantum optics is:

$$(S_1, S_2, S_3) \leftrightarrow (Z, X, Y), \quad (15)$$

corresponding to the $\{H, V\}$, $\{+, -\}$ and $\{L, R\}$ polarizations being the eigenstates of Z , X and Y respectively. Under this convention, a linear retarder, such as a waveplate, at an angle θ to the vertical axis, is described by the following matrix:

$$\begin{aligned} U(\theta) &= e^{-\frac{i}{2}\theta Y} e^{-\frac{i}{2}rZ} e^{\frac{i}{2}\theta Y} \\ &= \begin{bmatrix} \cos(\theta) & -\sin(\theta) \\ \sin(\theta) & \cos(\theta) \end{bmatrix} \begin{bmatrix} e^{\frac{i}{2}r} & 0 \\ 0 & e^{-\frac{i}{2}r} \end{bmatrix} \begin{bmatrix} \cos(\theta) & \sin(\theta) \\ -\sin(\theta) & \cos(\theta) \end{bmatrix} \end{aligned} \quad (16)$$

where r is the retardance of the element. Note that the matrix $U(\theta)$ is symmetric since:

$$\begin{aligned} U(\theta)^T &= (e^{\frac{i}{2}\theta Y})^T (e^{-\frac{i}{2}rZ})^T (e^{-\frac{i}{2}\theta Y})^T \\ &= e^{-\frac{i}{2}\theta Y} e^{-\frac{i}{2}rZ} e^{\frac{i}{2}\theta Y}. \end{aligned} \quad (17)$$

Propagating through such an element backwards has the effect of taking $\theta \rightarrow -\theta$. This transformation can be written as:

$$ZU(\theta)Z = U(-\theta) \quad (18)$$

since

$$Ze^{-\frac{i}{2}\theta Y}Z = e^{\frac{i}{2}\theta Y}. \quad (19)$$

For a general polarization gadget consisting of several linear retarders described by the unitary $U_{G, \text{fw}}$ in the forwards direction we find the unitary for the backwards propagation direction, $U_{G, \text{bw}}$, by transposing the order of the individual linear retarders and changing the sign of their respective angles:

$$U_{G, \text{fw}} = U_1(\theta_1) \dots U_n(\theta_n) \rightarrow U_{G, \text{bw}} = U_n(-\theta_n) \dots U_1(-\theta_1) \quad (20)$$

which can be written:

$$U_{G, \text{fw}} \rightarrow ZU_{G, \text{fw}}^T Z \quad (21)$$

since:

$$\begin{aligned} Z(U_1(\theta_1) \dots U_n(\theta_n))^T Z &= ZU_n(\theta_n) \dots U_1(\theta_1)Z \\ &= ZU_n(\theta_n)Z \dots ZU_1(\theta_1)Z \\ &= U_n(-\theta_n) \dots U_1(-\theta_1). \end{aligned} \quad (22)$$

The transformation in Eq. (21) is not useful for realising the transpose, since the Z gates around the unitary $U_{G, \text{fw}}^T$ have to be undone to recover the transpose. However, this problem can be overcome by picking a different convention for the polarization basis states, such as $(S_1, S_2, S_3) \leftrightarrow (X, Y, Z)$ which is a cyclic permutation of the aforementioned one (corresponding to a rotation of the basis vectors by $\pi/3$ around the vector $[1 \ 1 \ 1]$), and which is commonly used in polarimetry. In this work, we chose the convention:

$$(S_1, S_2, S_3) \leftrightarrow (-Z, -Y, -X). \quad (23)$$

The minus signs are necessary to preserve the handedness of the coordinate system when exchanging X and Y . That this convention yields the desired transformation under counterpropagation can be realised by noting that the

Stokes parameters of a unitary always transform as $(S_1, S_2, S_3) \rightarrow (S_1, -S_2, S_3)$, however for completeness we will perform the calculation explicitly. In the convention of Eq. (23) a linear retarder at an angle θ is written as:

$$U(\theta) = e^{\frac{i}{2}\theta X} e^{\frac{i}{2}rZ} e^{-\frac{i}{2}\theta X} \quad (24)$$

and the corresponding unitary in the backwards direction is

$$\begin{aligned} U(-\theta) &= e^{-\frac{i}{2}\theta X} e^{\frac{i}{2}rZ} e^{\frac{i}{2}\theta X} \\ &= (e^{\frac{i}{2}\theta X} e^{\frac{i}{2}rZ} e^{-\frac{i}{2}\theta X})^T \\ &= U(\theta)^T. \end{aligned} \quad (25)$$

It then follows that a general waveplate gadget also transforms as the transpose:

$$\begin{aligned} U_{G, \text{fw}} = U_1(\theta_1) \dots U_n(\theta_n) &\rightarrow U_{G, \text{bw}} = U_n(-\theta_n) \dots U_1(-\theta_1) \\ &= (U_1(\theta_1) \dots U_n(\theta_n))^T \\ &= U_{G, \text{fw}}^T. \end{aligned} \quad (26)$$

Sets of unitary operators used in the game

In this section, we explicitly list the two sets of unitary operators used in the discrimination task considered in this work. These sets of operators were first presented at Ref. [10].

$$\begin{aligned} \mathcal{M}_+ &:= \left\{ (I, I), (I, X), (I, Z), (X, I), (X, X), (X, Z), (Z, I), (Z, X), (Z, Z), \right. \\ &\quad \left. \left(\frac{X-Y}{\sqrt{2}}, \frac{X+Y}{\sqrt{2}} \right), \left(\frac{X+Y}{\sqrt{2}}, \frac{X-Y}{\sqrt{2}} \right), \left(\frac{Z-Y}{\sqrt{2}}, \frac{Z+Y}{\sqrt{2}} \right), \left(\frac{Z+Y}{\sqrt{2}}, \frac{Z-Y}{\sqrt{2}} \right) \right\} \\ \mathcal{M}_- &:= \left\{ (Y, I), (Y, X), (Y, Z), (I, Y), (X, Y), (Z, Y), \right. \\ &\quad \left. \left(\frac{I+iY}{\sqrt{2}}, \frac{I-iY}{\sqrt{2}} \right), \left(\frac{I-iY}{\sqrt{2}}, \frac{I+iY}{\sqrt{2}} \right) \right\}. \end{aligned} \quad (27)$$

Obtaining upper bounds for different classes of strategies

We now detail how to obtain an upper bound on the winning probability of the game described in the main manuscript. Let N be the total number of pairs of unitary operators contained in the set \mathcal{M}_+ and \mathcal{M}_- . Following a uniform distribution, i.e., with probability $1/N$, the referee picks a pair of unitary operators (U_i, V_i) . The player should then employ a quantum strategy to guess whether (U_i, V_i) belongs to \mathcal{M}_+ or \mathcal{M}_- . Let $p(\pm | (U_i, V_i))$ the probability that the player guesses $(U_i, V_i) \in \mathcal{M}_\pm$. The probability of such player to win the game is then given by

$$p = \frac{1}{N} \sum_{(U_i, V_i) \in \mathcal{M}_+} p(+ | (U_i, V_i)) + \sum_{(U_i, V_i) \in \mathcal{M}_-} p(- | (U_i, V_i)). \quad (28)$$

For the qubit scenario considered here, we can analyse the case where unitary gates act backwards by simply considering the case where all involved unitary operators are transposed. This is true because, as discussed earlier, there are only two anti-homomorphisms from $SU(d)$ to $SU(d)$, and for any $U \in SU(2)$, we have that $U^{-1} = \sigma_Y U^T \sigma_Y$. More explicitly, the winning probability for players using the unitary gates backwards is given by

$$p = \frac{1}{N} \sum_{(U_i, V_i) \in \mathcal{M}_+} p(+ | (U_i^T, V_i^T)) + \sum_{(U_i^T, V_i^T) \in \mathcal{M}_-} p(- | (U_i^T, V_i^T)). \quad (29)$$

Also, as we show more explicitly later, since the success probability is linear function of the strategies, convex combinations of forward and backwards strategies cannot increase the maximal success probability. Hence it is enough to analyse the forward and backwards case.

When the player is restricted to parallel strategies, the most general approach consists of preparing a quantum state ρ , sending part of this state to the operators U_i and V_i , and then performing a quantum measurement with outcomes labelled as $+$ or $-$, that is,

$$p_{\text{par}}(\pm | (U_i, V_i)) = \text{tr} \left[M_{\pm} \left(U_i \otimes V_i \otimes \mathbb{1} \right) \rho(U_i^\dagger \otimes V_i^\dagger \otimes \mathbb{1}) \right], \quad (30)$$

where $M_+, M_- \geq 0$ are the POVM operators associated to the outcomes $+$ and $-$, see Fig. 2 for a pictorial illustration.

Parallel strategies may be analysed in the (parallel) tester formalism [29, 47], also known as process POVM [48]. Let us label the linear spaces corresponding to the input and output spaces as \mathcal{H}_I and \mathcal{H}_O respectively. We can then write $U_i \otimes V_i : \mathcal{H}_I \rightarrow \mathcal{H}_O$ with $\mathcal{H}_I \cong \mathcal{H}_O \cong \mathbb{C}_2 \otimes \mathbb{C}_2$. In the tester formalism, operations are viewed as states and Eq. (30) may be written as the generalized Born's rule. More formally, we have that:

$$p_{\text{par}}(\pm | (U_i, V_i)) = \text{tr} \left[T_{\pm} |U_i \otimes V_i\rangle\langle U_i \otimes V_i| \right], \quad (31)$$

where¹ $T_+, T_- \in \mathcal{L}(\mathcal{H}_I \otimes \mathcal{H}_O)$ are tester elements and $|U_i \otimes V_i\rangle \in (\mathcal{H}_I \otimes \mathcal{H}_O)$ is the Choi vector of $U_i \otimes V_i$ defined as:

$$|U_i \otimes V_i\rangle := \sum_l |l\rangle \otimes (U_i \otimes V_i |l\rangle), \quad (32)$$

where $\{|l\rangle\}$ is the computational basis for \mathcal{H}_I . The operators T_+ and T_- are parallel testers when $T_+, T_- \geq 0$ and their sum respects:

$$T_+ + T_- = \sigma_I \otimes \mathbb{1}_O, \quad (33)$$

where $\sigma \in \mathcal{L}(\mathcal{H}_I)$ is a quantum state. As shown in Refs. [29, 47, 48], all parallel strategies as in Eq. (30) can be represented by testers such as those in Eq. (31), and *vice versa*. Hence, when optimizing over all possible strategies, instead of considering all possible states ρ and measurements M_{\pm} as in Eq. (30), we may optimize over all valid testers T_{\pm} as in Eq. (31).

One advantage of using the tester formalism, is that the maximal probability of winning the discrimination game can be written in terms of a semidefinite program (SDP) via the following optimisation problem:

$$\max \frac{1}{N} \left[\sum_{(U_i, V_i) \in \mathcal{M}_+} \text{tr} \left(T_+ |U_i \otimes V_i\rangle\langle U_i \otimes V_i| \right) + \sum_{(U_i, V_i) \in \mathcal{M}_-} \text{tr} \left(T_- |U_i \otimes V_i\rangle\langle U_i \otimes V_i| \right) \right] \quad (34)$$

$$\text{s.t.: } T_+, T_- \geq 0 \quad (35)$$

$$T_+ + T_- = \sigma_I \otimes \mathbb{1}_O \quad (36)$$

$$\text{tr}(\sigma) = 1. \quad (37)$$

Following the steps of Ref. [29], the dual problem is given by:

$$\min \text{tr}(C)/d_I \quad (38)$$

$$\text{s.t.: } \frac{1}{N} \sum_{(U_i, V_i) \in \mathcal{M}_+} |U_i \otimes V_i\rangle\langle U_i \otimes V_i| \leq C \quad (39)$$

$$\frac{1}{N} \sum_{(U_i, V_i) \in \mathcal{M}_-} |U_i \otimes V_i\rangle\langle U_i \otimes V_i| \leq C \quad (40)$$

$$\text{tr}_O(C) = \text{tr}_{IO}(C) \frac{\mathbb{1}_I}{d_I}, \quad (41)$$

¹ Here $\mathcal{L}(\mathcal{H}_I \otimes \mathcal{H}_O)$ denotes the set of linear operators from $\mathcal{H}_I \otimes \mathcal{H}_O$ (linear endomorphisms).

where d_I is the dimension of \mathcal{H}_I (for our particular problem, $d_I = 4$). By the definition of dual problem, if we find a linear operator C satisfying the feasibility constraints of inequality (39), inequality (40), and Eq. (41), the quantity $\text{tr}(C)/d_I$ is an upper bound on the maximal success probability. In order to obtain a computer-assisted-proof upper bound with fraction of integers, we use standard and efficient floating-point arithmetic algorithms to solve the SDP, obtain an operator C which satisfies the constraints of the dual problem and truncate it in such a way that the feasibility constraints are still satisfied. We refer to our online repository (see Code Availability) for an implementation of this procedure and to Ref. [29] for a detailed explanation on how to perform the truncation step.

When the player is restricted to causal strategies (also referred to as sequential strategies), the most general approach consists of preparing a quantum state ρ , sending part of this state to the operators U_i (or to V_i), applying a quantum channel \mathcal{E} , then performing the operation V_i (or U_i), and finally performing a quantum measurement with outcomes labelled as $+$ or $-$, that is:

$$p_{\text{seq}}(\pm|(U_i, V_i)) = \text{tr}\left[M_{\pm}(V_i \otimes \mathbb{1})\mathcal{E}\left(U_i \otimes \mathbb{1} \rho U_i^\dagger \otimes \mathbb{1}\right)(V_i^\dagger \otimes \mathbb{1})\right].$$

Using the concept of sequential testers [29, 47], we can also write the problem of finding the optimal causal strategy as an SDP. Since there is a notion of causal order, we label the input and output space of the first operation as \mathcal{H}_{I_1} and \mathcal{H}_{O_1} respectively. Analogously, we use \mathcal{H}_{I_2} and \mathcal{H}_{O_2} for the second operations. If the player uses the operation U_i first and V_i second, we have that $U_i : \mathcal{H}_{I_1} \rightarrow \mathcal{H}_{O_1}$ and $V_i : \mathcal{H}_{I_2} \rightarrow \mathcal{H}_{O_2}$. Following Ref. [29], the primal and dual problem for causal strategies are respectively given by

$$\max \frac{1}{N} \left[\sum_{(U_i, V_i) \in \mathcal{M}_+} \text{tr}\left(T_+ |U_i \otimes V_i\rangle\langle U_i \otimes V_i|\right) + \sum_{(U_i, V_i) \in \mathcal{M}_-} \text{tr}\left(T_- |U_i \otimes V_i\rangle\langle U_i \otimes V_i|\right) \right] \quad (42)$$

$$\text{s.t.: } T_+, T_- \geq 0 \quad (43)$$

$$T_+ + T_- = W_{I_1 O_1 I_2} \otimes \mathbb{1}_{O_2} \quad (44)$$

$$\text{tr}_{I_2}(W_{I_1 O_1 I_2}) = \sigma_{I_1} \otimes \mathbb{1}_{O_1} \quad (45)$$

$$\text{tr}(\sigma) = 1. \quad (46)$$

and

$$\min \text{tr}(C)/d_I \quad (47)$$

$$\text{s.t.: } \frac{1}{N} \sum_{(U_i, V_i) \in \mathcal{M}_+} |U_i \otimes V_i\rangle\langle U_i \otimes V_i| \leq C \quad (48)$$

$$\frac{1}{N} \sum_{(U_i, V_i) \in \mathcal{M}_-} |U_i \otimes V_i\rangle\langle U_i \otimes V_i| \leq C \quad (49)$$

$$\text{tr}_{O_2}(C) = \text{tr}_{I_2 O_2}(C) \otimes \frac{\mathbb{1}_{I_2}}{d_{I_2}} \quad (50)$$

$$\text{tr}_{O_1 I_2 O_2}(C) = \text{tr}_{I_1 O_1 I_2 O_2}(C) \frac{\mathbb{1}_{I_1}}{d_{I_1}}. \quad (51)$$

Another sequential strategy would be to use V_i before U_i . For this case, the semidefinite program is then exactly the same as the one before, but we exchange the roles of V_i and U_i . Our methods show that, when U_i precedes V_i , the success probability is bounded by $\frac{90}{100} \leq p_{UV} \leq \frac{91}{100}$, and when V_i precedes U_i , the success probability is bounded by $\frac{90}{100} \leq p_{VU} \leq \frac{91}{100}$. Since the two bounds coincide, we have $\frac{90}{100} \leq p_{\text{causal}} \leq \frac{91}{100}$.

When the player is restricted to general quantum strategies without a definite causal order, the strategies are described by means of an indefinite tester [30], which are positive semidefinite operators that add up to a process matrix [3], that is $T_+ + T_- = W$, where W is a bipartite process matrix. Following Ref. [29], and defining the

trace-and-replace maps as ${}_iX := \text{tr}_i(X) \otimes \mathbb{1}_i$, the primal and the dual problem are respectively given by

$$\max \frac{1}{N} \left[\sum_{(U_i, V_i) \in \mathcal{M}_+} \text{tr} \left(T_+ |U_i \otimes V_i\rangle\langle U_i \otimes V_i| \right) + \sum_{(U_i, V_i) \in \mathcal{M}_-} \text{tr} \left(T_- |U_i \otimes V_i\rangle\langle U_i \otimes V_i| \right) \right] \quad (52)$$

$$\text{s.t.: } T_+, T_- \geq 0 \quad (53)$$

$$T_+ + T_- = W \quad (54)$$

$$I_2 O_2 W = O_1 I_2 O_2 W \quad (55)$$

$$I_1 O_1 W = O_2 I_1 O_1 W \quad (56)$$

$$W = O_1 W + O_2 W - O_1 O_2 W \quad (57)$$

$$\text{tr}(W) = \text{tr}(\mathbb{1}_{O_1 O_2}). \quad (58)$$

and

$$\min \text{tr}(C)/d_I \quad (59)$$

$$\text{s.t.: } \frac{1}{N} \sum_{(U_i, V_i) \in \mathcal{M}_+} |U_i \otimes V_i\rangle\langle U_i \otimes V_i| \leq C \quad (60)$$

$$\frac{1}{N} \sum_{(U_i, V_i) \in \mathcal{M}_-} |U_i \otimes V_i\rangle\langle U_i \otimes V_i| \leq C \quad (61)$$

$$O_1 C = I_1 O_1 C \quad (62)$$

$$O_2 C = I_2 O_2 C. \quad (63)$$

Data analysis

As described in the main text, the game was played by having the referee pick pairs of unitaries from the sets \mathcal{M}_\pm in a uniformly random way in every round. The player's outcome was determined by the first unused photon detection event in the event list corresponding to that choice of unitary by the referee. More concretely, let $O_\pm^{j,k}$ be the k -th element in the time ordered list of detection events \mathcal{O}_\pm^j for the implemented pair of unitaries M_\pm^j . Then the outcome of the n -th round of the game, in which the referee picked the pair of unitaries M_\pm^j for the k -th time, is $O_\pm^{j,k}$.

In order to filter out background events resulting from various back-reflections in the experimental setup, as well as detector dark counts, two-fold coincidence events between the signal and idler photons were used to time filter the detection events.

The superconducting nanowire detectors used in the experiment have a slight polarization dependence in their detection efficiency, and due to the different pairs of unitaries generating different target qubit states the event rates for different implemented unitaries varied. This difference in efficiency was not necessary to account for, because the number of events for each pair of unitaries was truncated, in reverse chronological order, to match the setting with the fewest events. To find the numbers of rounds won and lost, the data was sampled from once, drawing 10^6 different samples from unique, chronologically ordered (for each setting) detection events. The exact number of won and lost rounds in this sampling were 994,512 won and 5,488 lost.

A detection efficiency imbalance is also present in the two output ports of the interferometer, corresponding to the two different measurement outcomes of the control qubit. This efficiency difference could quite easily be characterised and corrected for, however such actions are equivalent to classical post-processing and is captured by the indefinite tester. Imbalanced detection efficiency could therefore not lead to a violation of the bound, and is not necessary to correct for since the data already violates the bound.

The measurement of the fidelity between the unitary implemented in one direction and the transpose of the unitary in the other direction was performed with coherent light. To estimate the fidelity, the two unitaries were

first fitted to the data using a maximum likelihood estimation and then the fidelity was calculated by evaluated the following average:

$$\mathcal{F} = \langle (U_{fw}|\Psi\rangle)^\dagger U_{bw}^T |\Psi\rangle \rangle_{|\Psi\rangle}, \quad (64)$$

taken over 1000 Haar-random states $|\Psi\rangle$. This was done in every step of a Monte-Carlo simulation to estimate the measurement uncertainties induced by the waveplate errors.